Radiochim. Acta **89**, 357–362 (2001)

Excitation function of the $^{18}O(p,n)^{18}F$ nuclear reaction from threshold up to 30 MeV

By E. Hess[1], S. Takács[2], B. Scholten[1], F. Tárkányi[2], H. H. Coenen[1] and S. M. Qaim[1,*]

[1] Institut für Nuklearchemie, Forschungszentrum Jülich GmbH, D-52425 Jülich, Germany
[2] Institute of Nuclear Research of the Hungarian Academy of Sciences, H-4001 Debrecen, Hungary

(Received November 10, 2000; accepted in revised form January 30, 2001)

Nuclear reaction / Excitation function / Integral yield / Enriched target / ^{18}F-production / Positron emitter

Summary. The available experimental data on the most common route for the production of ^{18}F, viz. $^{18}O(p,n)^{18}F$ reaction, obtained both via neutron spectral studies and activation measurements, were critically reviewed. In some energy regions the cross section database was found to be rather weak or discrepant. In order to fill the gaps and to clear some of the discrepancies, the excitation function was remeasured from threshold up to 30 MeV using different solid and gas targets containing highly enriched ^{18}O. For this purpose a van de Graaff machine ($E_p < 4$ MeV) and several cyclotrons ($E_p = 4$–30 MeV) were utilized. The new experimental data help to prepare a recommended data set. At $E_p = 14$ MeV the integral yield of ^{18}F calculated from the new excitation curve is slightly higher than that from the hitherto accepted data set; at $E_p > 14$ MeV the yields reported here are new.

1. Introduction

The radioisotope ^{18}F ($T_{1/2} = 109.7$ min; $I_{\beta^+} = 97\%$; $E_{\beta^+} = 0.63$ MeV) is the most commonly used radionuclide in Positron Emission Tomography (PET). This is due to the relatively long half-life and lowest β^+ energy among the major PET radioisotopes, viz. ^{11}C, ^{13}N, ^{15}O and ^{18}F. The low β^+ energy leads to high-resolution scans and the relatively long half-life allows the transportation of ^{18}F-labelled radiopharmaceuticals over several hundred kilometres as well as measurement of slow pharmacokinetics.

Fluorine-18 has been found to be useful also as a source of slow positron beams [cf. 1]. Formation of light mass radioactive nuclei and their decay via radiative neutron capture is of astrophysical interest. A knowledge of the production yields of those radioisotopes is thus of significance for developing radioactive beams [cf. 2] The reaction cross sections and ^{18}F-yields are also important for determining the oxygen impurity in various materials via charged particle activation analysis [cf. 3].

The production methods of ^{18}F have been reviewed several times [cf. 4–7]. Out of all the reactions investigated, the $^{20}Ne(d,\alpha)^{18}F$ and the $^{18}O(p,n)^{18}F$ processes have been commonly utilized. In recent years the $^{18}O(p,n)^{18}F$ reaction on highly enriched ^{18}O-targets (both gaseous and $H_2{}^{18}O$) has been extensively used. However, considering the importance of this reaction, the cross section database is not well established.

Recently a detailed compilation of the available experimental data on the $^{18}O(p,n)^{18}F$ reaction was done in the framework of an IAEA Coordinated Research Project (CRP) entitled: "Charged Particle Cross Section Database for Medical Radioisotope Production". Results of both neutron studies [8–14] and activation measurements [3, 15–19] were considered. The data were then critically analysed and an effort was made to evaluate them. In this regard, the predictive power of nuclear theory was found to be very low and one had to resort to some fitting procedures to be able to give a recommended curve. Evidently, the quality of such a curve depended strongly on the quality of the available data. The results are to be published in a TECDOC [20]. In specific terms, it was ascertained that

– very few activation data exist in the low energy region (< 4 MeV) which has gained some significance in view of the newly proposed low energy accelerators,
– the database at energies > 15 MeV is very weak,
– there are some discrepancies between the activation and neutron measurements.

The cross sections reported by Ruth and Wolf [19] are presently considered to be standard data for ^{18}F production via the $^{18}O(p,n)^{18}F$ reaction. However, in view of the above mentioned deficiencies, we decided to remeasure the excitation function covering the full energy range from threshold up to 30 MeV. We were aware of the fact that using the activation technique it is not easy to improve the quality of an excitation function having a well resolved resonance structure. The work demanded a good energy resolution of the bombarding beam and a well defined target thickness. A knowledge of the real number of target nuclei has great importance in cross section work. In this regard, important factors are density reduction in the gas target, and uniformity and composition of the solid target. The measurement of the activity of the positron emitting ^{18}F may involve contributions from some other positron emitters. In spite of these difficulties we thought the new data would contribute usefully to solving the basic discrepancies.

*Author for correspondence (E-mail: s.m.qaim@fz-juelich.de).

2. Experimental

Cross sections were measured using the stacked-gas cell and stacked-foil techniques at the compact cyclotron CV 28 and the injector of COSY of the Forschungszentrum Jülich GmbH (FZJ). Furthermore, single solid targets were irradiated at the van de Graaff machine and the MGC-20E cyclotron of the ATOMKI, Debrecen. In order to meet different technical conditions at those accelerators and due to the need of thin targets in measuring cross sections at low energies, enriched ^{18}O-targets were prepared in three different chemical forms, namely $^{18}O_2$, $Si^{18}O_2$ and $Al_2{}^{18}O_3$.

2.1 Target preparation

Enriched $^{18}O_2$ gas was supplied by Chemotrade, Leipzig (Germany). Its isotopic composition and chemical purity are given in Table 1. The gas was filled into stainless steel cells (diameter 2 cm, length 2.5 cm) having 100 μm aluminium windows which were attached to the gas cells using rubber O-rings and tightened with screws. The gas pressure varied between 0.4 and 1.5 bar, resulting in weight per unit area as 1.8×10^{-3} to 7.0×10^{-3} g/cm^2. The gas filling apparatus and procedure have been described earlier [21].

$Si^{18}O_2$ powder with an ^{18}O enrichment of 95% (cf. Table 1) was supplied by Chemotrade, Leipzig (Germany). Targets were prepared using the sedimentation technique. About 5 mg of the powder was suspended in a solution of 2.5 mg Levapren© (polyethylenevinylacetate) in 2 ml dichloromethane. The suspension was transferred to a sedimentation cell (diameter 1.2 cm, height 2.5 cm). At the bottom of the cell an aluminium foil was attached and tightened with an O-ring and screws. At ambient temperature, the solvent evaporated slowly and the $Si^{18}O_2$ together with the polymer got deposited on the aluminium foil. The polymer was necessary to obtain higher mechanical stability of the $Si^{18}O_2$ deposit. After further drying at 100 °C the targets were ready for irradiation. The weight including the Levapren© was $6.1–7.3 \times 10^{-3}$ g/cm^2. The deposits appeared as homogeneous on visual inspection; at 50 times magnification under a microscope, however, some small inhomogeneities were observed. This was taken into consideration in the error estimation.

$Al_2{}^{18}O_3$ targets were prepared by electrochemical oxidation of aluminium. This method is established in the aluminium industry to passivate aluminium workpieces [22]. It was adopted for the purpose of thin target preparation.

Table 1. Composition of targets used.

Target	Isotopic composition [%]	Weight per unit area [mg/cm^2]
$^{18}O_2$	^{18}O $(96.7 \pm 0.3)^a$ ^{17}O $(1.1 \pm 0.1)^a$ ^{16}O $(2.2 \pm 0.2)^a$ chemical purity > 99.9% $O_2{}^a$	1.8–7.0
$Si^{18}O_2$	^{18}O $(95 \pm 3)^a$	6.1–7.3
$Al_2{}^{18}O_3$	^{18}O $(83 \pm 5)^b$	1.9–4.7

a: values given by the supplier;
b: measured via SIMS.

The electrochemical oxidation was performed in an electrolytic cell described earlier [23]. The electrolyte consisted of ∼ 2 g enriched water (ISOTEC, USA, ^{18}O-enrichment > 97%) and 0.4 g conc. sulphuric acid, giving sulphuric acid with a concentration of 20%. The electrolyte was stirred by a rotating platinum cathode. As anode a 50 μm aluminium foil was attached at the bottom of the cell. The electrolysis was carried out with a voltage of 16–18 V, resulting in a current of 14–17 mA over a time varying between 30 min and 2 h. An ICP-MS analysis showed that 1–2 mg aluminium from the anode foil was dissolved in the sulphuric acid during electrolysis. Therefore, it was not possible to estimate the amount of oxygen converted to $Al_2{}^{18}O_3$ simply by weighing. The $Al_2{}^{18}O_3$ layer had to be separated from the aluminium by dissolving the unreacted aluminium with 0.5 ml conc. hydrochloric acid. $Al_2{}^{18}O_3$ is insoluble in this acid and stayed back as a thin film which was successively washed with water and ethanol, dried and weighed. Finally, the $Al_2{}^{18}O_3$ was fixed on an aluminium foil using one drop of a 5% solution of polystyrene in toluene. After evaporation of toluene and further drying at 100 °C, the targets were subjected to secondary-ion mass-spectrometry (SIMS), which allows mass analysis of solid surfaces. The ^{18}O-enrichment of those targets was found to be $83 \pm 5\%$ (cf. Table 1). The weight including the polymer was in the range of 1.9×10^{-3} to 4.7×10^{-3} g/cm^2 of the deposit. No inhomogeneities were observed in the deposits even at 50 times magnification.

2.2 Irradiations and beam current monitoring

Irradiations in the low energy region up to 7 MeV were carried out at the van de Graaff machine and the MGC-20E cyclotron in Debrecen. For this purpose the thin $Al_2{}^{18}O_3$ targets were used. Only one target at a time was irradiated. No additional foil for beam monitoring was used because of two reasons: (a) too much energy loss and (b) lack of a suitable monitor reaction. Each irradiation was carried out with a proton beam current of about 100 nA for about 30 min. The incident proton energies were varied in 100–200 keV steps from 2.7 up to 4.1 MeV and in 500 keV steps from 5 to 7 MeV. The beam current was measured via a Faraday cup.

At the compact cyclotron CV 28 in Jülich, $^{18}O_2$ gas cells as well as $Al_2{}^{18}O_3$ and $Si^{18}O_2$ targets were bombarded. Not more than two gas cells or three oxide targets were irradiated in a stack. The cyclotron vacuum was separated from the gas cells with a 50 μm titanium foil. Copper foils (10–25 μm) were used to monitor the beam current and to degrade the incident proton energy. Irradiations were carried out for 5 to 15 min with beam currents of 100 nA. The primary incident proton energies applied were 7.0 ± 0.2, 12.0 ± 0.2, 16.0 ± 0.2 and 21.0 ± 0.2 MeV. The total energy degradation in a stack was not more than 3 MeV.

At the injector of the cooler synchrotron (COSY) in Jülich experiments were carried out with $Si^{18}O_2$ and $Al_2{}^{18}O_3$ targets. Three of these targets were stacked together with copper and titanium foils for beam current monitoring and energy degradation. The energy difference between the first and the third target was not more than 5 MeV. The proton beam current used was between 200 and 300 nA and the irradiation time in each case was 15 min. The primary

proton energy at the injector was well known from the adjusted beam extraction parameters [24] and was in each case 45.6 ± 0.2 MeV. This energy was degraded via absorber foils to about 30 MeV, which then served as incident energy for the first target sample. By choosing the $^{nat}Cu(p, xn)^{62}Zn$ and $^{nat}Ti(p, xn)^{48}V$ processes as monitor reactions (see below) and adopting the monitor ratio method for determining the effective projectile energy at a given position in the stack [cf. 25], the proton energy incident on the first target sample was estimated. This value agreed with the calculated degraded value within ± 0.5 MeV. We took this uncertainty into account while estimating the energy scale error.

The beam currents in the irradiations at CV 28 and the injector were measured with Faraday cups as well as via monitor reactions. For proton energies up to 20 MeV the $^{nat}Cu(p, xn)^{63}Zn$ process and for higher energies the $^{nat}Cu(p, xn)^{62}Zn$ and $^{nat}Ti(p, xn)^{48}V$ reactions were used. For these reactions evaluated and recommended data exist [26]. A summary of the irradiation facilities used is given in Table 2. The mean energies and the energy degradations in the targets were calculated according to Williamson *et al.* [27].

2.3 Measurement of radioactivity

The radioactivity of each reaction and monitor product was determined via γ-ray spectrometry using HPGe detectors. Counting of foils and solid oxide targets was done at varying distances between 10 and 50 cm. In case of gas targets, measurements were done at a large source to detector distance of about 50 cm. Due to the fact that ^{18}F has no characteristic γ-line, its activity had to be determined via a decay curve analysis of the 511 keV annihilation peak. Positrons were annihilated in 2 mm thick copper sheets placed on both sides of an irradiated target. The minimum required thickness of the copper sheet for complete absorption of the positron energy was calculated using Bethe's stopping power formula and Sternheimer's theory of the density effect [28]. The calculation took into consideration the maximum positron energy of ^{22}Na, which is 1.8 MeV. This nuclide was used as a standard source for estimating the detector efficiency for the 511 keV annihilation peak. The calculation resulted in a minimum thickness of 1.6 mm. With a thickness of 2 mm all positrons emitted from ^{22}Na as well as ^{18}F should be stopped and annihilated within the copper sheet.

Counting was generally started about 100 min after EOB to allow short-lived products like ^{13}N ($T_{1/2} = 10$ min) and ^{15}O ($T_{1/2} = 2$ min) to decay. Nuclides with half-lives longer than ^{18}F were observed only in the spectra of a few samples irradiated with intermediate energy protons. They were identified via their γ-rays as ^{55}Co ($T_{1/2} = 17.4$ h) and ^{52}Mn ($T_{1/2} = 5.6$ d). In those cases only ^{55}Co was considered in the 511 keV decay curve analysis since the small count rates of ^{52}Mn merge in the background (Fig. 1). Both nuclides probably originate from (p, xn) reactions on traces of iron and chromium in the aluminium foils.

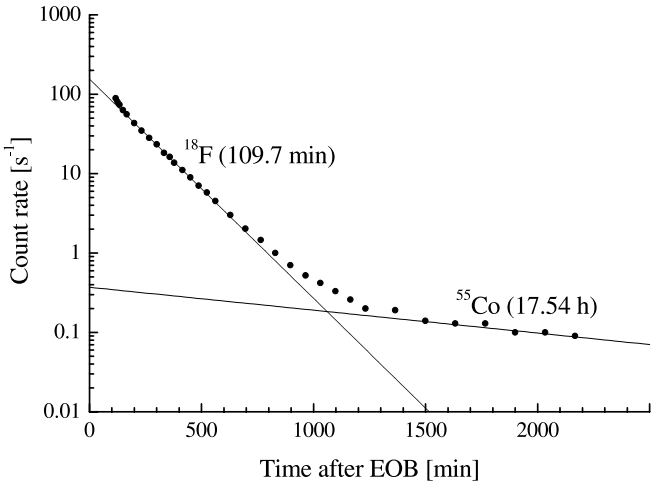

Fig. 1. Decay curve analysis of the annihilation peak from an $Al_2{}^{18}O_3$-target bombarded with 24.6 MeV protons. Measurement was started about 1.5 h after the end of bombardment to allow complete decay of short-lived components like nitrogen-13, oxygen-15 etc.

2.4 Calculation of cross sections and their errors

From the measured decay rates of the radioactive product ^{18}F and the measured beam currents, the cross sections were calculated using the standard activation formula. The total error in the measured cross section was obtained by combining the individual errors in quadrature. The major individual errors were: proton beam intensity via Faraday cup at the van de Graaff and MGC-20E (1%), monitor reactions (10%), detector efficiency (5%), peak area analysis and counting statistics (5%–9%). The error in the number of ^{18}O-nuclei depended on the kind of target used and was as follows: $^{18}O_2$ (error in ^{18}O-enrichment 0.5%, target pressure 5%, density reduction by beam heating 5%), $Si^{18}O_2$ (error in ^{18}O-enrichment 3%, inhomogeneity 10%), and $Al_2{}^{18}O_3$ (error in ^{18}O-enrichment 5%, inhomogeneity 5%).

The error in the energy scale was estimated from the absorption of protons in the target. Uncertainties in the primary proton energy and the target thicknesses were taken into account in this error estimation. Depending on the spread of the primary proton energy, the extent of energy degradation in the stack and the thicknesses of the individual samples, the energy error ranged between 2% and 10%. The highest errors occurred at the lowest energies in a stack.

Table 2. Irradiation facilities used.

Energy range	Accelerator	Targets used	Beam current monitoring
2.7–4 MeV	van de Graaff, Debrecen	$Al_2{}^{18}O_3$	Faraday cup
5–7 MeV	MGC-20E, Debrecen	$Al_2{}^{18}O_3$	Faraday cup
4–21 MeV	CV 28, Jülich	$^{18}O_2$, $Si^{18}O_2$, $Al_2{}^{18}O_3$	Monitor reaction
20–30 MeV	Injector of COSY, Jülich	$Si^{18}O_2$, $Al_2{}^{18}O_3$	Monitor reaction

3. Results and discussion

In this work about 110 cross section data points were determined using three different ^{18}O-targets at four different accelerators. The results are given in Table 3. The errors range between 7 and 18%. The data fill the gaps in the hitherto known database, especially in the low energy region from threshold up to 4 MeV and at energies above 15 MeV.

The data on the $^{18}O(p,n)^{18}F$ reaction now available are shown in Fig. 2. The energy region up to 12 MeV is presented on an expanded scale in Fig. 3. Compared with the neutron data [cf. 9–11], our activation measurements are not able to resolve the structure of the excitation function between 3 and 4.5 MeV containing several very small resonances. For this purpose the targets used were not thin enough. In spite of this drawback, our cross sections consti-

Table 3. Measured cross sections of the $^{18}O(p,n)^{18}F$ reaction.

Proton energy [MeV]	Cross section [mb]	Accelerator Target[a]	Proton energy [MeV]	Cross section [mb]	Accelerator Target
2.43 ± 0.23	3.6 ± 0.4	A 3	7.04 ± 0.5	217.9 ± 25.7	C 1
2.52 ± 0.23	4.6 ± 0.5	A 3	7.37 ± 0.4	312.1 ± 50.8	C 2
2.56 ± 0.12	13.5 ± 1.6	A 3	7.60 ± 0.5	226.8 ± 33.2	C 1
2.65 ± 0.21	5.9 ± 0.7	A 3	7.60 ± 0.4	249.2 ± 40.0	C 3
2.75 ± 0.21	8.1 ± 1.0	A 3	8.10 ± 0.4	192.1 ± 23.3	C 1
2.77 ± 0.11	6.9 ± 0.8	A 3	8.19 ± 0.4	232.7 ± 34.0	C 3
2.85 ± 0.12	9.4 ± 1.0	A 3	8.58 ± 0.4	270.5 ± 39.6	C 3
2.86 ± 0.28	25.4 ± 3.0	A 3	8.77 ± 0.4	261.9 ± 38.3	C 3
2.91 ± 0.16	25.7 ± 3.0	A 3	9.04 ± 0.3	273.3 ± 44.5	C 2
2.97 ± 0.21	30.1 ± 3.5	A 3	9.10 ± 0.3	257.9 ± 37.7	C 3
3.07 ± 0.19	47.3 ± 5.6	A 3	9.10 ± 0.4	214.4 ± 26.0	C 1
3.13 ± 0.19	55.8 ± 6.6	A 3	9.64 ± 0.3	238.4 ± 34.9	C 3
3.18 ± 0.26	51.2 ± 6.0	A 3	9.74 ± 0.3	240.4 ± 39.1	C 2
3.28 ± 0.14	45.5 ± 5.4	A 3	10.11 ± 0.3	198.1 ± 32.2	C 2
3.34 ± 0.25	40.2 ± 4.7	A 3	10.46 ± 0.3	153.7 ± 18.4	C 1
3.43 ± 0.14	45.3 ± 5.3	A 3	10.49 ± 0.3	186.0 ± 27.2	C 1
3.49 ± 0.18	31.1 ± 3.7	A 3	10.49 ± 0.3	201.0 ± 29.3	C 1
3.49 ± 0.10	31.7 ± 3.7	A 3	10.74 ± 0.3	207.5 ± 33.8	C 2
3.54 ± 0.20	69.0 ± 11.2	C 2	10.77 ± 0.3	186.0 ± 27.2	C 3
3.59 ± 0.18	34.7 ± 4.1	A 3	10.94 ± 0.3	201.8 ± 32.9	C 2
3.62 ± 0.30	67.0 ± 8.2	C 1	11.21 ± 0.3	193.7 ± 31.5	C 2
3.65 ± 0.17	35.0 ± 4.1	A 3	11.33 ± 0.3	165.6 ± 26.4	C 2
3.69 ± 0.18	60.2 ± 7.1	A 3	11.55 ± 0.3	179.1 ± 29.2	C 2
3.69 ± 0.09	47.3 ± 5.6	A 3	12.26 ± 0.4	122.6 ± 14.6	C 1
3.80 ± 0.17	88.3 ± 10.4	A 3	12.69 ± 0.3	134.1 ± 21.8	C 2
3.85 ± 0.20	45.6 ± 7.4	C 2	13.26 ± 0.3	118.0 ± 14.6	C 1
3.87 ± 0.19	92.3 ± 10.9	A 3	13.37 ± 0.3	136.0 ± 19.9	C 1
4.19 ± 0.2	175.0 ± 25.5	C 1	13.84 ± 0.3	120.2 ± 19.6	C 2
4.30 ± 0.3	146.2 ± 23.8	C 2	14.06 ± 0.3	94.2 ± 11.2	C 1
4.56 ± 0.2	221.7 ± 32.4	C 1	14.12 ± 0.3	141.7 ± 20.7	C 1
4.57 ± 0.3	178.8 ± 26.2	C 3	14.27 ± 0.3	129.8 ± 21.1	C 2
4.59 ± 0.3	265.3 ± 42.6	C 3	14.50 ± 0.3	72.1 ± 8.6	C 1
4.81 ± 0.3	202.5 ± 29.6	C 3	15.33 ± 0.3	98.1 ± 1.6	C 2
4.91 ± 0.3	218.3 ± 25.7	B 3	16.01 ± 0.5	59.5 ± 7.1	C 1
4.96 ± 0.3	219.3 ± 26.2	C 1	16.22 ± 0.4	74.5 ± 8.8	C 1
5.02 ± 0.3	585.9 ± 85.5	C 1	16.93 ± 0.4	61.0 ± 8.9	C 1
5.04 ± 0.3	392.6 ± 57.4	C 3	17.30 ± 0.4	44.6 ± 6.5	C 1
5.25 ± 0.3	412.0 ± 60.1	C 1	17.42 ± 0.4	54.9 ± 8.0	C 1
5.35 ± 0.3	458.6 ± 54.1	B 3	17.72 ± 0.4	43.7 ± 5.2	C 1
5.46 ± 0.3	404.6 ± 65.0	C 3	17.95 ± 0.4	66.6 ± 9.7	C 1
5.65 ± 0.3	494.1 ± 72.1	C 1	18.01 ± 0.4	50.3 ± 6.0	C 1
5.85 ± 0.3	258.4 ± 30.5	B 3	18.18 ± 0.3	62.5 ± 9.1	C 1
5.94 ± 0.4	248.5 ± 36.3	C 3	18.20 ± 0.3	37.9 ± 5.5	C 1
6.12 ± 0.3	250.6 ± 40.8	C 2	18.65 ± 0.3	45.1 ± 6.6	C 1
6.21 ± 0.3	221.9 ± 36.1	C 2	19.04 ± 0.3	53.5 ± 7.8	C 1
6.24 ± 0.4	312.5 ± 50.2	C 3	19.34 ± 0.3	45.7 ± 5.4	C 1
6.26 ± 0.3	185.2 ± 21.8	B 3	19.58 ± 1.2	24.1 ± 3.5	D 3
6.27 ± 0.4	231.2 ± 33.8	C 3	19.93 ± 0.3	33.0 ± 4.8	C 1
6.47 ± 0.4	234.5 ± 34.3	C 3	20.51 ± 0.2	54.6 ± 8.0	C 1
6.73 ± 0.3	141.0 ± 23.0	C 2	21.63 ± 1.0	28.2 ± 4.1	D 3
6.75 ± 0.3	147.8 ± 21.6	C 3	22.93 ± 0.9	32.5 ± 4.8	D 3
6.78 ± 0.4	166.7 ± 24.4	C 3	24.49 ± 0.8	23.3 ± 3.4	D 3
6.86 ± 0.4	199.7 ± 23.5	B 3	26.46 ± 0.8	26.4 ± 4.3	D 2
6.90 ± 0.3	237.0 ± 34.7	C 3	28.31 ± 0.7	18.3 ± 2.7	D 3
6.94 ± 0.4	217.2 ± 34.9	C 3	30.02 ± 0.6	29.0 ± 4.7	D 2

a: abbreviations: A: van de Graaff, B: MGC-20E, C: CV 28, D: injector of COSY; 1: $^{18}O_2$, 2: $Si^{18}O_2$, 3: $Al_2{}^{18}O_3$

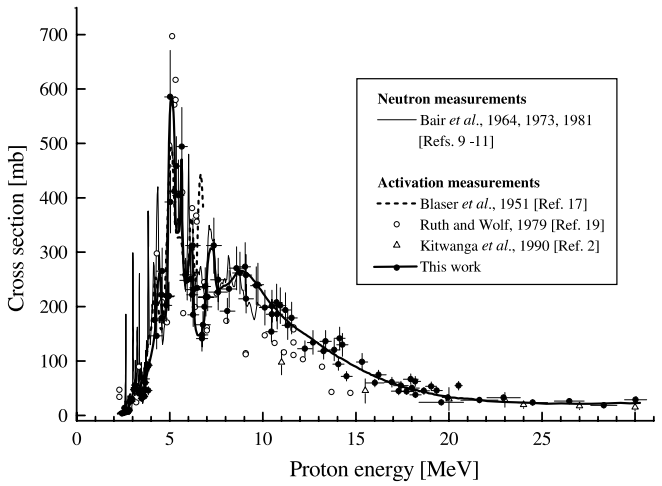

Fig. 2. Excitation function of the $^{18}O(p, n)^{18}F$ reaction. Results of both neutron and activation measurements are shown. The rather bold curve is an eye-guide to our activation data.

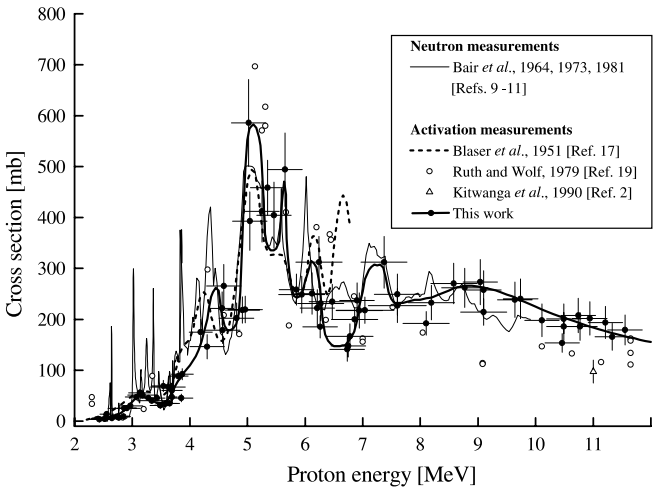

Fig. 3. Excitation function of the $^{18}O(p, n)^{18}F$ reaction in the energy range of 2 to 12 MeV shown on an expanded scale. The bold curve is an eye-guide to our activation data.

tute a more complete database for ^{18}F yield calculation. On the other hand, the resonances with a relatively large half-width, e.g. at 5.1, 6.1 and 7.2 MeV, could be resolved and are in agreement with the neutron data.

As regards the literature activation data, our cross sections between 4 and 8 MeV are in good agreement with the data of Ruth and Wolf [19]. Below 4 MeV very few activation data have been reported. Above 8 MeV our cross sections are slightly higher but still seem to be within the statistical errors of the values reported by Ruth and Wolf. The four cross section values at 11.65 MeV measured by them are 111, 134, 158 and 162 mb. The maximum cross section value is in absolute agreement with our result. Worth pointing out is the absence of the resonance at 6.8 MeV reported by Blaser *et al*. [17]. Neither Ruth and Wolf nor we could confirm it. As far as the results of Kitwanga *et al*. [2] are concerned, our cross sections are in good agreement above 20 MeV. At lower energies the data of Kitwanga *et al*. are lower, possibly due to the rather thick gas targets used by them.

The integral yields calculated from our cross section curve up to an energy of about 8 MeV are in reasonable agreement with those reported by Ruth and Wolf [19]. Above that energy our yield becomes increasingly higher; at 14 MeV the difference is about 15%. The results are depicted in Fig. 4. The yield above 14 MeV is presented here for the first time. Since some groups may intend to use the new yield data as reference points in optimisation of their targets, we give in Table 4 the numerical values of saturation yields of ^{18}F and ranges of respective incident proton energies in 100% enriched ^{18}O. If an $H_2{}^{18}O$ target is used, the ^{18}F-yield would be about

Table 4. Saturation yields[a] of ^{18}F via the $^{18}O(p, n)^{18}F$ reaction.

Proton energy [MeV]	Yield [MBq/μA]	Range [mg/cm^2]	Proton energy [MeV]	Yield [MBq/μA]	Range [mg/cm^2]
2.4	1.07	0.9	10.5	7495	157.1
2.6	3.73	2.7	11.0	8080	170.7
2.8	12.7	4.8	11.5	8736	185.3
3.0	19.9	6.8	12.0	9157	201.3
3.2	52.7	9.1	12.5	9760	217.5
3.4	71.5	11.2	13.0	10 140	234.1
3.6	81.3	13.8	13.5	10 672	250.7
3.8	124	16.4	14.0	11 004	268.7
4.0	164	18.9	14.5	11 407	286.5
4.5	471	26.4	15.0	11 765	305.6
5.0	836	33.5	16.0	12 423	344.7
5.5	1632	41.7	17.0	12 978	385.7
6.0	2209	50.5	18.0	13 454	428.6
6.5	2677	60.0	19.0	13 871	473.9
7.0	3036	70.0	20.0	14 228	520.4
7.5	3730	80.2	21.0	14 547	568.6
8.0	4222	91.7	22.0	14 853	619.1
8.5	4962	104.6	24.0	15 532	733.0
9.0	5513	115.9	26.0	16 060	849.5
9.5	6345	129.9	28.0	16 555	975.6
10.0	6871	142.2	30.0	17 132	1110.9

a: calculated from the excitation function curve given in Fig. 2 (related to 100% enrichment of ^{18}O).

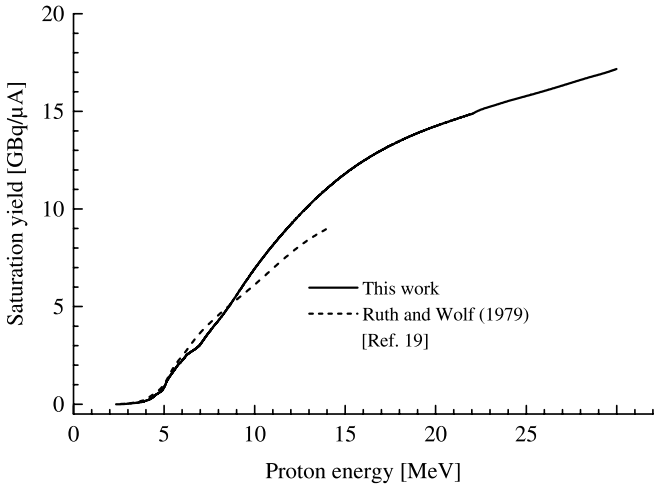

Fig. 4. Calculated saturation integral yield of fluorine-18 as a function of proton energy from 100% enriched ^{18}O.

17% lower. Worth pointing out is that the yield at $E_p \leq 4$ MeV is appreciably lower than the value [19] based on an interpolation of the limited literature data in this energy region.

Acknowledgment. This research was partly supported by the Deutsche Forschungsgemeinschaft (DFG), Bonn (Grant QA 1/1-1). Part of the work was also done under a German-Hungarian bilateral agreement (No. HUN 98/027). We are grateful to the staff of the four accelerators used for their cooperation. The ICP-MS and SIMS analyses of $Al_2{}^{18}O_3$ samples were kindly done at the Zentralabteilung für Chemische Analysen (ZCH) of the Forschungszentrum Jülich.

References

1. Nozaki, T., Itoh, Y., Peng, Z. L., Nakanashi, N., Goto, A., Ito, Y., Yoshida, H.: Preparation of ^{18}F source for slow positron beam by proton bombardment of ^{18}O-water. J. Radioanalyt. Nucl. Chem. **239**, 175 (1999).
2. Kitwanga, S., Leleux, P., Lipnik, P.: Production of $^{14,15}O$, ^{18}F and ^{19}Ne radioactive nuclei from (p, n) reactions up to 30 MeV. Phys. Rev. C **42**, 748 (1990).
3. Krasnov, N. N., Dmitriyev, P. P., Dmitriyeva, S. P, Konstantinov, I. O., Molin, G. A.: Experimental data on the yields of ^{11}C, ^{13}N, ^{18}F isotopes used for the detection of carbon, nitrogen, oxygen and neighbouring light element impurities by means of activation analysis with different charged particles (p, d, ^3He, α). Proc. Conf. *The Use of Cyclotrons in Chemistry, Metallurgy and Biology*. (Amphlett, C. B., Ed.), Oxford, September (1969), Butterworths, London, p. 341.
4. Qaim, S. M., Stöcklin, G.: Production of some medically important short-lived neutron deficient radioisotopes of halogens. Radiochim. Acta **34**, 25 (1983).
5. Qaim, S. M.: Recent developments in the production of ^{18}F, $^{75,76,77}Br$ and ^{123}I. Appl. Radiat. Isot. **37**, 803 (1986).
6. Guillaume, M., Luxen, A., Nebeling, B., Argentini, M., Clark, J. C., Pike, V. W.: Recommendations for fluorine-18 production. Appl. Radiat. Isot. **42**, 749 (1991).
7. Qaim, S. M., Clark, J. C., Crouzel, C., Guillaume, M., Helmke, H. J., Nebeling, B., Pike, V. W., Stöcklin, G.: PET-radionuclide production. In: *Positron Emission Tomography-Methodology Aspects*. (Stöcklin, G., Pike, V. W., Eds.), Kluwer, Dardrecht, The Netherlands (1993), pp. 1-42.
8. Hill, H. A., Blair, J. M.: Yields of the $^{18}O(p, \alpha)^{15}N$ and $^{18}O(p, n)^{18}F$ reactions for protons of 800 keV to 3500 keV. Phys. Rev. **104**, 198 (1956).
9. Bair, J. K., Jones, C. M., Willard, H. B.: Neutrons from the proton bombardment of ^6Li, ^7Li, ^9Be, ^{11}B and ^{18}O. Nucl. Phys. **53**, 209 (1964).
10. Bair, J. K.: Total neutron yields from the proton bombardment of $^{17,18}O$. Phys. Rev. C **8**, 120 (1973).
11. Bair, J. K., Miller, P. D., Wieland, B. W.: Neutron yields from the 4–12 MeV proton bombardment of ^{11}B, ^{13}C and ^{18}O as related to the production of ^{11}C, ^{13}N and ^{18}F. Int. J. Appl. Radiat. Isot. **32**, 389 (1981).
12. Anderson, J. D., Bloom, S. D., Wong, C., Hornyak, W. F., Madsen, V. A.: Effective two-body force inferred from the (p, n) reaction on ^{17}O, ^{18}O, ^{27}Al and other light nuclei. Phys. Rev. **177**, 1416 (1969).
13. Mark, H., Goodman, C.: Angular distribution of neutrons from $^{18}O(p, n)^{18}F$ reaction. Phys. Rev. **101**, 768 (1956).
14. Nagiar, V., Roclawski-Conjeaud, M., Szteinznaider, D., Thirion, J.: Reaction $^{18}O(p, n)^{18}F$ et niveaux du fluor 18. Compt. Rend. **242**, 1443 (1956).
15. DuBridge, L. A., Barnes, S. W., Bouk, J. H., Strain, C. V.: Proton induced radioactivities. Phys. Rev. **53**, 447 (1938).
16. Blaser, J. P., Boehm, F., Marmier, P., Preiswerk, P., Scherrer, P.: Fonctions d'excitation de la réaction $^{18}O(p, n)^{18}F$. Helv. Phys. Acta **22**, 598 (1949).
17. Blaser, J. P., Boehm, F., Marmier, P., Scherrer, P.: Fonctions d'excitation de la réaction (p, n) (III) éléments légers. Helv. Chim. Acta **24**, 465 (1951).
18. Blair, J. M., Leigh, J. J.: Total cross sections of the $^{18}O(p, \alpha)^{15}N$ and $^{18}O(p, n)^{18}F$ reactions. Phys. Rev. **118**, 495 (1960).
19. Ruth, T. J., Wolf, A. P.: Absolute cross sections for the production of ^{18}F via $^{18}O(p, n)^{18}F$ reaction. Radiochim. Acta **26**, 21 (1979); Erratum: Radiochim. Acta **42**, 219 (1987).
20. Qaim, S. M., Tárkányi, F., Takács, S., Hermanne, A., Nortier, M., Oblozinsky, P., Scholten, B., Shubin, Y. N., Zhuang, Y.: Positron emitters. In: *Charged Particle Cross Section Database for Medical Radioisotope Production*. IAEA-TECDOC-1211, Vienna (2001) pp. 231–277.
21. Tárkányi, F., Qaim, S.M., Stöcklin, G.: Excitation functions of ^3He- and α-particle induced nuclear reactions on enriched ^{82}Kr and ^{83}Kr. Radiochim. Acta **43**, 185 (1988).
22. Ullmanns Encyklopädie der technischen Chemie. 4. neubearbeitete und erweiterte Auflage, Band 12, Verlag Chemie, Weinheim, New York (1996).
23. Mushtaq, A., Qaim, S. M.: Excitation functions of α- and ^3He-particle induced nuclear reactions on natural germanium: evaluation of production routes for ^{73}Se. Radiochim. Acta **50**, 27 (1990).
24. Blessing, G., Bräutigam, W., Böge, H. G., Gad, N., Scholten, B., Qaim, S. M.: Internal irradiation system for excitation function measurement via the stacked-foil technique. Appl. Radiat. Isot. **46**, 955 (1995).
25. Piel, H., Qaim, S. M., Stöcklin, G.: Excitation functions of (p, xn)-reactions on ^{nat}Ni and highly enriched ^{62}Ni: possibility of production of medically important radioisotope ^{62}Cu at a small cyclotron. Radiochim. Acta **57**, 1 (1992).
26. Tárkányi, F., Takács, S., Gul, K., Hermanne, A., Mustafa, M. G., Nortier, M., Oblozinský, P., Qaim, S. M., Scholten, B., Shubin, Y. N., Zhuang, Y.: Beam monitor reactions. In: *Charged Particle Cross Section Database for Medical Radioisotope Production*. IAEA-TECDOC-1211, Vienna (2001) pp. 47–150.
27. Williamson, C. F., Boujot, J. P. Picard, J.: *Tables of range and stopping power of chemical elements for charged particles of energy* 0.5 *to* 500 MeV. Report CEA-R 3042 (1966).
28. Seltzer, S. M., Berger, M. J.: Improved procedure for calculating the collision stopping power of elements and compounds for electrons and positrons. Int. J. Appl. Radiat. Isot. **35**, 665 (1984).